

Evaluating the ability of satellite-based quantitative precipitation estimates to resolve heavy precipitation amounts over 1, 3 and 6-hour intervals

Yu Zhang^{1*}, Dongsoo Kim², Robert Kuligowski³

¹Office of Hydrologic Development, NOAA National Weather Service, Silver Spring MD

²NOAA National Climatic Data Center, Asheville, NC

³Center for Satellite Applications and Research, NOAA National Environmental Satellite, Data, & Information Service, Camp Spring, MD

1. INTRODUCTION

Flash flood monitoring and prediction (FFMP) is one of the key functions of NOAA's National Weather Service (NWS). At present, FFMP is commonly based on radar/rain gauge multi-sensor quantitative precipitation estimates (QPEs). In areas outside of effective radar coverage or with a sparse rain gauge network, satellite precipitation estimates (SPEs) can supplement ground-sensor based QPEs for FFMP (Kondragunta et al., 2005). There are two potential roles of SPEs in this respect. The first is to serve as a basis for determining the rainfall climatology in areas with poor radar/rain gauge coverage, and the second is to detect in real time the heavy precipitation events with high flooding potential in conjunction with the SPE-based rainfall climatology. An element of rainfall climatology that is particularly useful for this purpose is the precipitation amount with the Annual Exceedance Probability (AEP) of 0.5 – bank-full flow has an AEP of roughly 0.5 (Reed et al. 2007). Although gridded estimates of precipitation frequency are available for a large portion of the U.S. from NOAA Atlas 14 (Bonnin et al., 2006) and its various volumes, the availability of the SPE values corresponding to 0.5 AEP is still valuable in that SPE may suffer from bias (Zhang et al., 2010) and this bias can be offset by using SPE-based PFEs in the same manner as in Distributed Hydrologic Model – Threshold Frequency (DHM-TF) approach (Reed et al. 2007). Therefore, SPE-based PFEs would provide a good context for judging the flooding potential of storms as seen from the satellites (Personal communication, Sheldon Kusselson at National Environmental Satellite, Data and Information Service, Satellite Analysis Branch).

To date, there is a body of literature on climate applications of SPE (e.g., Ferraro 1997, Xie and Arkin, 1995). Yet, few of the studies used SPE as the basis for deriving PFEs. Our study fills this gap by exploring the use of SPE for deriving the PFEs that could be used as thresholds for

detecting large rainfall amounts with substantial flash flood potentials. We designed an experiment and performed it in two phases over 22 catchments in Texas and Louisiana (Fig. 1) with size range from 218 to around 1975 km² (Table 1). The first phase entailed deriving two sets of PFEs using the mean areal precipitation (MAP) time series for each catchment, with the first based on the SPE produced using the Self-calibrating Multivariate Precipitation Retrieval (SCaMPR) algorithm and the second on West Gulf River Forecast Center (WGRFC) multisensor QPE (MQPE). The latter were then used as the reference to assess the accuracy in the former. In the second phase, the two sets of PFEs were used as thresholds in conjunction with respective QPEs to identify the events, i.e., instances where these thresholds were exceeded for respective QPEs. The events derived from SCaMPR SPE were compared with those from MQPE to examine the potential skill of SCaMPR for flash flood applications.

2. DATA AND METHODOLOGY

2.1 SCaMPR and Multi-sensor QPE

The SCaMPR algorithm was developed by Kuligowski (2002) in recognition of the shortcomings in algorithms solely based on GOES infrared brightness temperature (T_b). The SCaMPR algorithm has been scheduled by NOAA National Environmental Satellite, Data and Information Service (NESDIS) to replace the Hydro-Estimator (H-E) as the operational SPE algorithm. The SCaMPR framework still relies on T_b in three GOES infrared channels (6.9, 10.7 and 12.0 or 13.3 μm) as predictors of rain rates, but uses recent passive microwave (PMW) SPEs from Low Earth Orbital and Polar Orbiting Satellites, as well as those from the Tropical Rainfall Measuring Mission (TRMM; Kummerow et al., 1998) as a reference for calibrating the T_b to rain rate relationship. The calibration process involves first

using TRMM Precipitation Radar QPE to bias-correct the PMW QPEs from the TRMM Microwave Imager, and those from the Advanced Microwave Sounding Unit (AMSU) and Special Sensor Microwave Imager (SSM/I). The adjusted PWM QPEs then were used as predictors to calibrate the T_b to rainfall relationship via discriminant analysis and multiple regression.

Our reference for assessing the SCaMPR SPE is the multi-sensor QPEs from the NWS West Gulf River Forecast Center (WGRFC). The MQPEs are hourly gridded precipitation amounts on the Hydrologic Rainfall Analysis Project (HRAP) grid mesh (approx. 4km in dimension). This data set was created using primarily rain gauge and radar observations, and it incorporates extensive manual quality control. Although MQPE has been shown to be highly reliable for hydrologic forecasting, past studies suggest that it is subject to temporally varying bias (Zhang et al., 2011). To address this issue, we followed the technique of Zhang et al. (2011) and performed retrospective adjustments to the MQPEs to match calendar month total precipitation derived from rain gauge reports through PRISM-based interpolation (Daly et al., 1994).

In our work, the mean areal precipitation (MAP) time series were computed from the adjusted MQPEs and the SCaMPR SPEs for 22 catchments in the forecast domains of WGRFC for the period of 2000-7. The hourly MAP series were aggregated into 3- and 6-h intervals. For each of the MAP time series, the eight largest amounts were picked to form a partial duration time series (PDS) which served as the basis for deriving the PFEs.

2.3 Deriving Precipitation Frequency Estimates

The PFEs were derived by assuming that they follow the Generalized Extreme Value (GEV) distribution. The cumulative density function (CDF) of GEV takes the following form:

$$F(x) = \exp\left\{\left[1 - \frac{k}{a}(x - \xi)\right]^{1/k}\right\} \text{ if } k \neq 0$$

$$= \exp\left\{-\exp\left[-\frac{1}{a}(x - \xi)\right]\right\} \text{ if } k = 0$$

where x is the precipitation amount, and ξ , α , and k are location, scale, and shape parameters, respectively.

The precipitation amount corresponding to a given exceedance probability is

$$x = F^{-1}\left(\frac{1}{1-p}\right)$$

where p is the AEP. Note $p=0.5$ for a 2-year return event.

The GEV parameters were estimated for each MAP series by applying the L-moment method to the PDS. L-moment (Hosking, 1990) is a method widely used in the precipitation frequency literature and it has been shown to perform well for small sample sizes. For GEV, the first three L-moments are

$$\lambda_1 = \xi + \frac{\alpha}{k}(1 - \Gamma(1+k))$$

$$\lambda_2 = \frac{\alpha}{k}(1 - 2^{-k})(1 - \Gamma(1+k))$$

$$\lambda_3 = \frac{2(1 - 3^k)}{(1 - 2^k)} - 3$$

Where $\Gamma()$ is the CDF of the gamma distribution. The sample L-moments (computed from the PDS) were used to compute the GEV parameters, and the resultant GEV distributions were applied to derive the PFEs.

3. RESULTS

3.1 Comparison of PFEs

The 2-Year PFEs derived from SCaMPR SPE and adjusted MQPEs on 1, 3 and 6-h intervals are shown in Figure 2 for each catchment.

The comparisons reveal a substantial low bias in the 1-h SPE-based PFEs relative to those based on MQPEs, and a tendency for the bias to improve towards longer time intervals. The correlation between the SPE and MQPEs, computed by lumping values from multiple catchments, was high for 1-h PFEs and lower for the longer time intervals. At the 1-h interval, the correlation is 0.85 and the percentage bias (PB) is 24% (PB is defined as the ratio of the difference to the PFEs based on MQPE); for the 6-h PFEs, the

correlation dropped to 0.50 whereas bias is nearly neutral (0.3%). While an earlier study by Zhang et al. (2010) points to the overall positive bias in the SCA-MPR SPE relative to MQPEs, it is clear that, from a distribution standpoint, the 1-h SCA-MPR SPE-based MAP underrepresents large precipitation amounts as observed in MQPE. Meanwhile, it also appears that the underestimation is quite consistent among catchments at the 1-h interval so that a high degree of correlation is achieved despite the bias. At longer intervals, the underestimation on the average becomes less severe. In fact the PFEs from SCA-MPR SPEs are equal to or exceed those from MQPEs for several catchments, and the number of these basins are higher at 6-h than at 3-h. Yet at these intervals, the differences in PFEs from SPEs and MQPEs become a lot larger across basins, leading to lower correlation.

The geographic distribution of the PFEs is illustrated in Figure 4, where the 3-h results from SPE and MQPE are shown. On an overall basis, the two sets of PFEs show visible resemblance. However, it is evident that the PFEs from SPE are not able to replicate some small-scale spatial variations as seen over the basins clustered along the Texas-Louisiana border.

3.2 Dependence of estimated PFE on estimated mean annual rainfall

The relationship between PFEs and annual precipitation amounts is characterized in Figure 4, where PFEs from SPE and MQPEs are plotted against the mean annual precipitation based on the respective data set over the 8-year period. Overall both sets of PFEs are significantly correlated with the precipitation amounts. Between the two, the correlation values are mostly higher for MQPEs. Another notable observation is that, for MQPEs, correlation tends to improve towards longer time intervals (from 0.65 at 1-h to 0.69 at 3-h and 0.70 at 6-h). Such a feature is not observed for SPE, for which the correlation is rather high at 3-h (0.70) but is much lower for 1 and 6-h (0.52 and 0.54, respectively).

The fact the PFEs and the precipitation totals are correlated points to the potential of improving the SPE-based PFEs via bias correction of SPE. However, SCA-MPR SPE, as shown in the study by Zhang et al. (2010), is subject to a positive overall bias. It is likely that a simple bias correction would further lower the PFEs on an overall basis while

improving the across-basin consistency against PFEs from MQPE. Therefore a more sophisticated adjustment of the entire PDF might be warranted.

3.3 The Detection Experiment

A detection experiment was carried out to examine SPE skill in detecting heavy precipitation episodes, by coupling SPE with SPE-based PFEs. In this experiment, both SPE and MQPE values were compared with their respective PFEs to identify the events, i.e., the time intervals where the PFE was exceeded. Note that a time window three times the length of the accumulation period was allowed in determining successful detection by SPE. For example, a 1-h event at 1000UTC on July 1, 2004 was determined using MQPE. A successful detection was registered if a SPE rainfall event occurred anywhere between 0900 and 1100UTC. Table 1 shows the number of events as derived from MQPE and the number among which that were successfully detected using SPE for each basin.

On a multi-basin average basis, the detection rate is low. At 1-h, only 9 out of 92 events were correctly identified using SPE. The rate improves only slightly at 3 and 6-h intervals, where 10 out of 89 (3-h) and 92 (6-h) were identified. Out of the 22 catchments, successful detection of at least one event was observed in 8 catchments regardless of time intervals. Only in one catchment, RPIL1, were a majority of events detected at 3-h and 6-h intervals (3 out of 5). The 3-h MQPE and SCA-MPR-based MAP series for RPIL1 and the identified events are shown in Figure 5. A closer examination reveals that three of the events identified using MQPE were clustered between June 16 and 17 of 2006. Two of the three events were successfully detected using SCA-MPR SPE.

4. SUMMARY AND PRELIMINARY CONCLUSIONS

We experimented with using SCA-MPR SPE for deriving Precipitation Frequency Estimates (PFEs) to aid the detection of storms with flooding potential in areas with poor radar and rain gauge coverage. In our study, two sets of PFEs were computed for 22 WGRFC catchments from 1-h, 3-h and 6-h Mean Areal Precipitation (MAP) series based on SCA-MPR SPE and Multi-sensor QPE. Comparisons between the SPE and MQPE-based

PFEs for 2-Year AEP reveal a close correlation between the two sets of values, and a negative bias of the former at 1-h interval. For 3- and 6-h accumulations, the bias diminishes but the correlation also drops. Since SCaMPR SPE exhibits a positive overall bias, simple bias correction is unlikely to improve the bias of PFEs at 1-h and more research on correcting conditional bias is needed in this respect. It was also found that PFEs closely correlate with mean annual precipitation amounts. This implies a potential of improving the cross-basin consistency in PFEs by performing climatologic adjustments of MAPs.

In the detection experiment, SCaMPR SPE and MQPE were coupled with corresponding PFEs to delineate the heavy precipitation events where the 1, 3, and 6-h precipitation amounts exceed the respective PFEs. Our analyses indicate that detection rate remains low for SCaMPR SPE (around 10% for all three time scales), pointing to the need for further improvements in SPE algorithm in order to properly represent the relatively rare storm events.

Our results are promising but more work needs to be done to improve the accuracy of satellite-based PFEs and to extract the maximum value from satellite-based PFEs when deriving multi-sensor PFEs. While large discrepancies remain between the heavy precipitation events as represented by SPE versus those by MQPEs, it appears that the availability of a reference set of areal-average PFEs would be a useful aid in interpreting the significance of unusually large SPE-indicated accumulations. It should be noted that, due to the short duration of the record, there is substantial uncertainty with respect to the PFEs from the SPEs and the MQPEs. Additional studies are underway to quantify the uncertainty. In addition, it needs to be noted that the PFEs can differ substantially from those documented in Atlas 14, and their use should be restricted to the storm detection application as illustrated in this paper.

5. ACKNOWLEDGEMENTS

We appreciate the assistance of Gregory Shelton and Robert Corby from West Gulf River Forecasts Center in supplying the multisensor QPEs. This work also benefited from conversations with meteorologists at NESDIS Satellite Analysis Branch and forecasters at WGRFC.

7. REFERENCES

- Bonnin, G. and co-authors, 2006: NOAA Atlas 14. Precipitation-Frequency Atlas of the United States, Silver Spring, MD (Available from <http://www.nws.noaa.gov/oh/hdsc/currentpf.htm>)
- Daly, C., R. P. Neilson, and D. L. Phillips, 1994: A statistical-topographic model for mapping climatological precipitation over mountainous terrain. *J. Clim. Appl. Meteorol.*, 33, 140–158.
- Ferraro, R. R., 1997: Special sensor Microwave Imager derived global rainfall estimates for climatological applications. *J. Geophys. Res.*, 102, 16715-16735.
- Hosking J. R. M., 1990: L-moments: analysis and estimation of distributions using linear combinations of order statistics. *J. of the Royal Statistical Society, Series B*, 52, 105-124.
- Kondragunta C. and co-authors, 2005: Objective integration of satellite, rain gauge, and radar precipitation estimates in the Multisensor Precipitation Estimator algorithm. *Preprints, 19th Conference on Hydrology*, San Diego, Amer. Meteor. Soc., 2.8.
- Kuligowski, R. J., 2002: A self-calibrating GOES rainfall algorithm for short-term rainfall estimates. *J. Hydrometeorol.*, 3, 112-130.
- Kummerow, C., W. Barnes, T. Kozu, J. Shiue, and J. Simpson, 1998: The Tropical Rainfall Measuring Mission (TRMM) sensor package. *J. Atmos. Ocean. Technol.*, 15, 808–816.
- Reed, S., J. Schaake, and Z. Zhang, 2007: A distributed hydrologic model and threshold frequency-based method for flash flood forecasting at ungauged locations. *J. Hydrology*. 337, 402-420.
- Xie, P. and P. Arkin, 1995: An intercomparison of gauge observations and satellite estimates of monthly precipitation. *J. Clim. Appl. Meteorol.*, 34, 1143–1160.
- Zhang, Y., and co-authors, 2010: Evaluation of the impacts of ingesting TRMM data on the

accuracy of quantitative precipitation estimates obtained via the SCaMPR framework. *Preprints, 24th Conference on Hydrology*, San Diego, Amer. Meteor. Soc, 72–75.

Zhang, Y., S. Reed, and D. Kitzmiller, 2011: Effects of retrospective gauge-based readjustment of multisensor precipitation estimates on hydrologic simulations. *J. Hydromet.*, 12, 429–443.

Table 1. The Detection of Precipitation Events at 1, 3 and 6-h intervals by SCaMPR SPE

Catchment	Size (km ²)	1-h		3-h		6-h	
		Total ¹	Success ²	Total	Success	Total	Success
QLAT2	218	5	1	5	1	3	1
GNAV2	266	4	0	4	0	5	0
SDAT2	326	3	0	3	0	4	0
RSRT2	417	4	0	6	0	4	0
MCKT2	439	5	0	3	0	5	0
MTPT2	447	4	1	3	0	4	0
LYNT2	519	4	0	5	0	3	0
SKMT2	611	4	0	3	0	5	0
CRKT2	650	4	0	4	0	3	0
SOLT2	678	4	2	4	0	4	0
BRVT2	814	4	0	3	1	4	1
MDST2	868	5	0	4	0	4	0
SBMT2	919	3	0	5	1	4	1
RPIL1	932	5	1	5	3	4	3
SCDT2	935	3	0	3	0	5	0
BWRT2	988	4	0	4	1	4	1
DWYT2	993	4	0	3	1	4	1
TDDT2	1107	4	2	5	1	5	1
ATBT2	1262	5	1	4	1	6	1
LOLT2	1492	5	0	4	0	4	0
REFT2	1795	4	1	4	0	5	0
UVAT2	1975	5	0	5	0	3	0
Total		92	9	89	10	92	10

1 Total number of events identified based on MQPE.

2 The number of events successfully detected by SCaMPR out of those identified by MQPE.

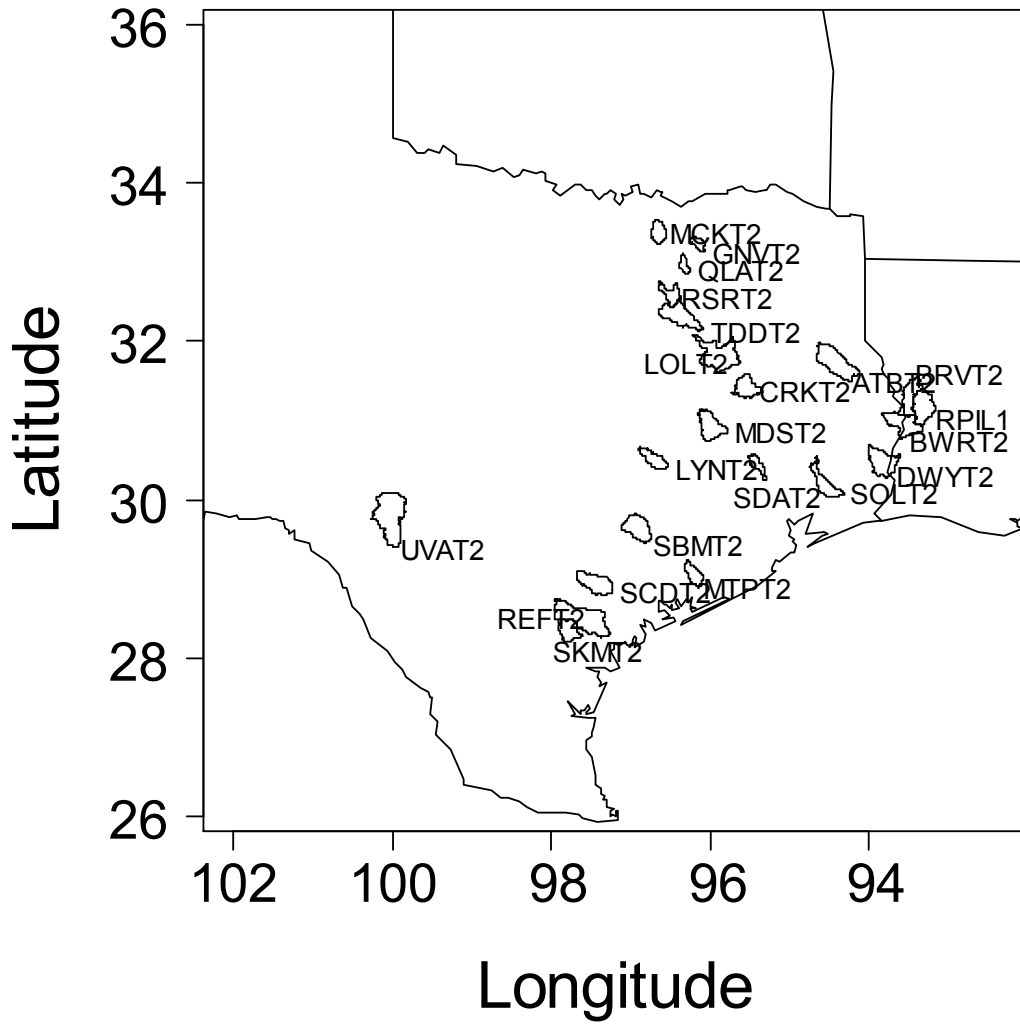


Figure 1: 22 study catchments in West Gulf River Forecast Center (WGRFC) domain.

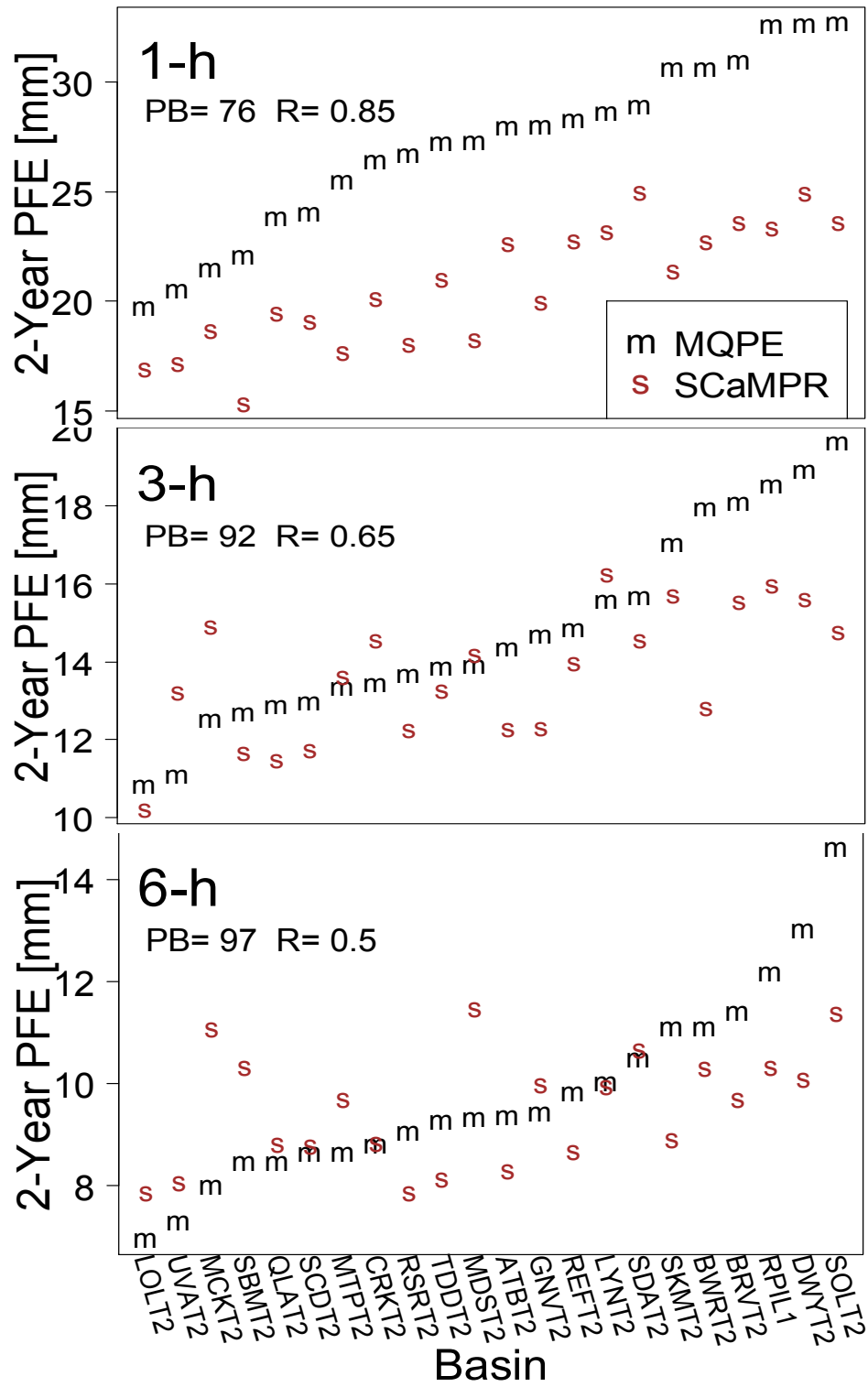
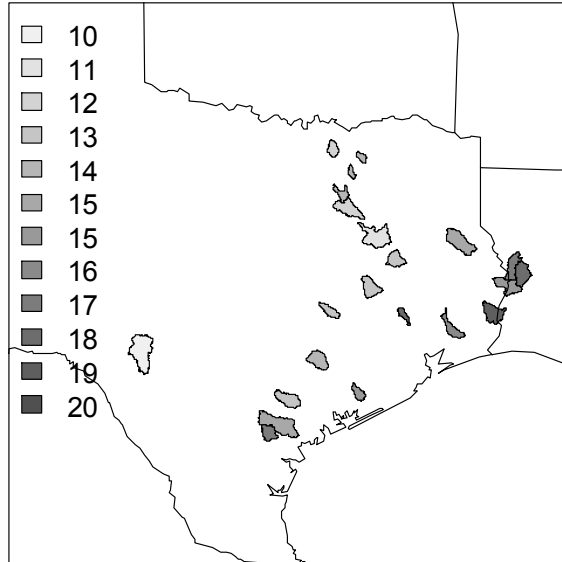


Figure 2: Precipitation Frequency Estimates (PFEs) computed using MQPE and SCaMPR SPE at 1, 3, and 6-h scales.

a) WG MQPE



b) SCaMPR SPE

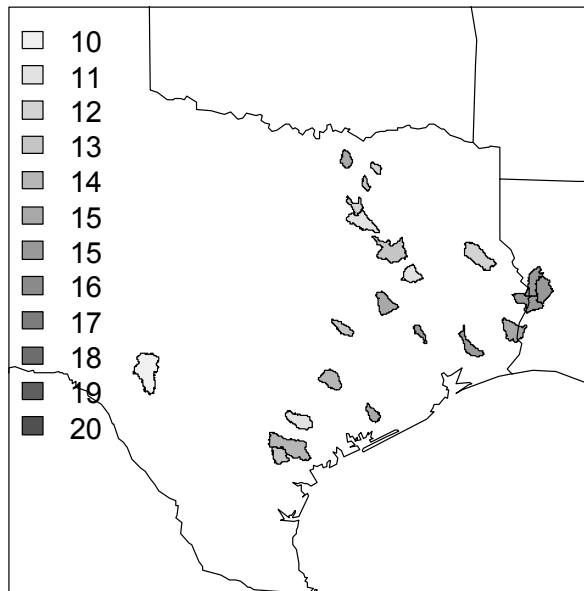
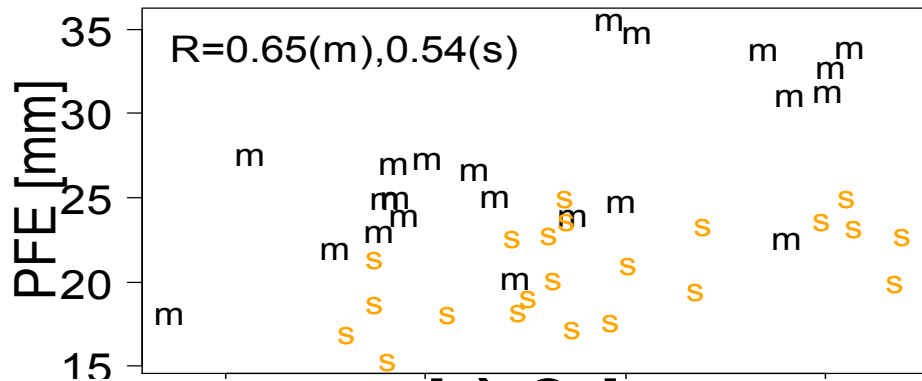
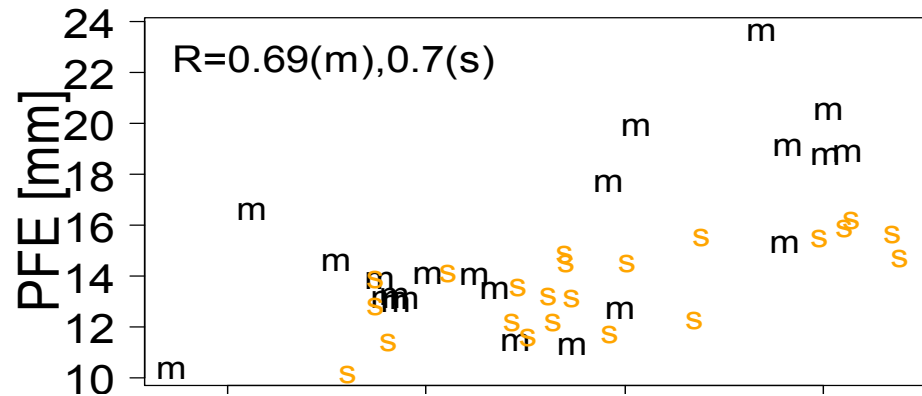


Figure 3: 3-h Precipitation Frequency Estimates (PFEs) for 0.5 AEP based on a) WGRFC MQPE, and b) SCaMPR SPE.

a) 1-h



b) 3-h



c) 6-h

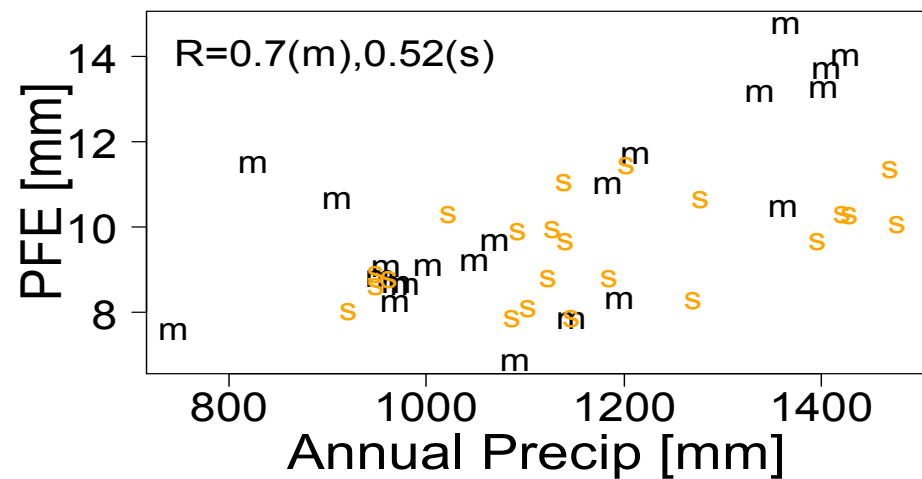


Figure 4: Comparisons of MQPE and SPE-based PFE associated with 0.5 AEP versus mean annual precipitation from PRISM for a) 1-h, b) 3-h, and c) 6-h intervals. Superimposed are correlation values for MQPE (m) and SCA-MPR SPE (s).

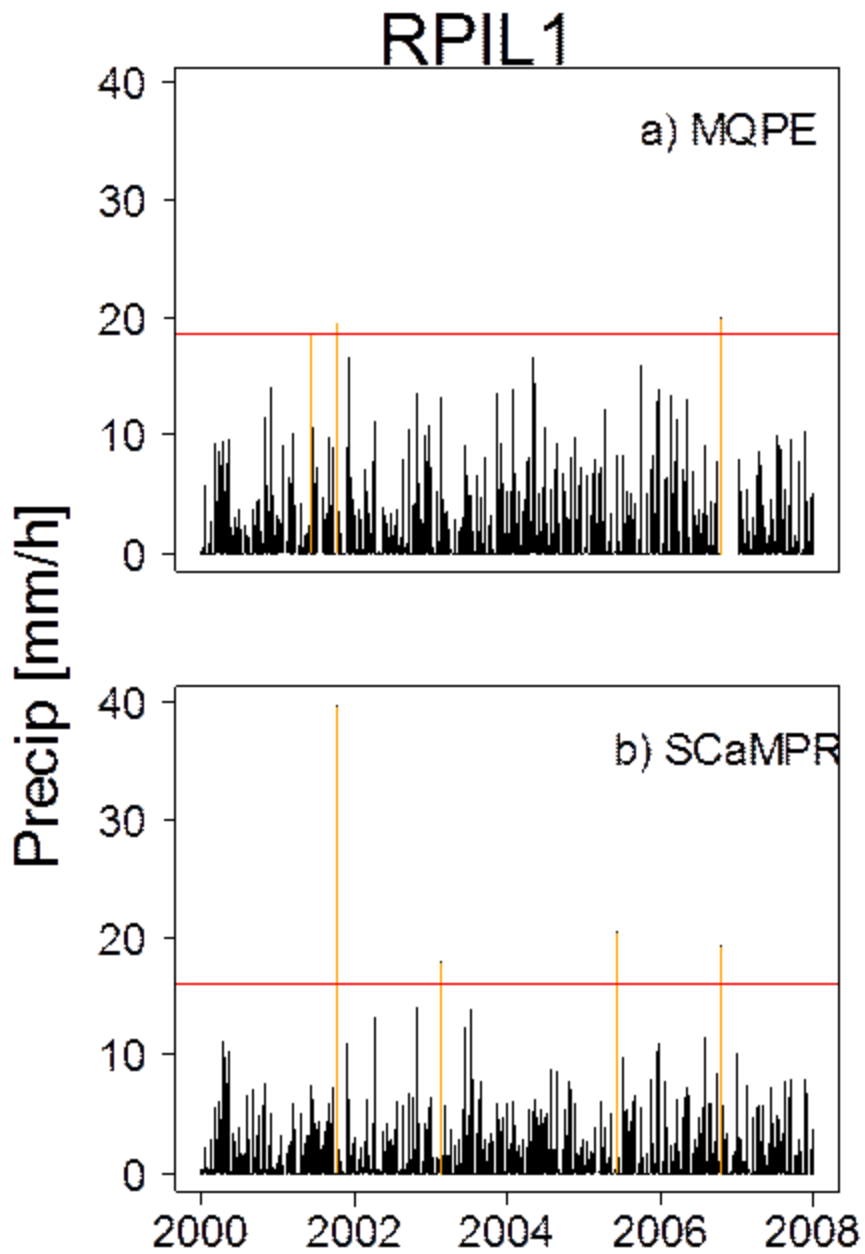


Figure 5: Events where 3-h precipitation exceeds the PFEs corresponding to the 0.5 AEP as depicted by a) MQPE and b) SCaMPR SPE for catchment RPIL1. Note that three events are clustered in June 2007 in a). Two of the three events were successfully detected using SCaMPR SPE.